ISSN1027-5495. Functional Materials, 32, No.1 (2025), p. 87-96
doi:http://dx.doi.org/10.15407/fm32.01.87 © 2025 — STC "Institute for Single Crystals"

Low-cost ceramic membrane supports based on ukrainian kaolin and saponite

Y. Molchan, L. Bohdan, S. Kyrii, O. Tymoshenko, I. Pylypenko, A. Burmak, G. Vasyliev, T. Dontsova

National Technical University of Ukraine "Igor Sikorsky Kyiv Polytechnic Institute", 37, Prospect Beresteiskyi, Kyiv 03056, Ukraine

Received September 1, 2024

The synthesis of ceramic membranes using natural raw materials, especially kaolin and saponite clays, is a rational approach to reducing the cost of ceramic membranes for water purification. This study investigated the effect of sintering temperature and phase composition of the initial mixture on the physicochemical, mechanical, and transport properties of ceramic membranes based on kaolin and saponite. The initial clay components and ceramic membrane matrices obtained from them were characterised using diffraction methods, FTIR and thermal analysis. It was shown that the kaolin phase primarily determines the structural-adsorption characteristics of the ceramic membrane matrices. The determined mechanical properties indicate a significant influence of temperature and composition of the initial mixture on the flexural strength limit, with the selected ceramic matrices being in the range of 10–16 MPa. The electrical properties suggest potential resistance to contamination during operation. The revealed a macroporous structure of the obtained membranes provides their good permeability for pure water.

Keywords: ceramic membrane supports, kaolin, saponite, mechanical and transport properties.

Низьковартісні керамічні мембранні матриці на основі українського каоліну та сапоніту. *Ю. Молчан, Л. Богдан, С. Кирій, О. Тимошенко, І. Пилипенко, А. Бурмак, Г. Васильєв, Т. Донцова*

Синтез керамічних мембран з використанням природної сировини, а саме каоліну та сапонітової глини, є раціональним підходом до зниження вартості керамічних мембран для очищення води. В роботі досліджено вплив температури спікання та фазового складу вихідної суміші на фізико-хімічні, механічні та транспортні властивості керамічних мембран на основі каоліну та сапоніту. Вихідні глинисті компоненти та отримані з них матриці керамічних мембран були охарактеризовані за допомогою дифракційних методів досліджень, ІЧ-спектроскопії та термічного аналізу. Показано, що структурно-адсорбційні характеристики керамічних мембранних матриць визначається в основному властивостями каоліну. Одержані механічні властивості вказують на значний вплив температури та складу вихідної суміші на міцність на згин, яка для обраних керамічних матриць знаходиться в межах 10–16 МПа. Встановлені електричні властивості свідчать про потенційну стійкість до забруднення під час експлуатації, а транспортні властивості – про макропористу структуру отриманих мембран та їх достатньо високу проникність за чистою водою.

1. Introduction

Currently, membrane technologies are among the most versatile methods for water purification. Membranes made from polymeric materials, such as regenerated cellulose, polypropylene, polyamide, and polyvinyl chloride, have gained widespread popularity [1, 2]. These materials primarily dominate in wastewater treatment due to their low cost, ease of controlling mass exchange characteristics, and surface hydrophobicity. However, they have several drawbacks, such as limited lifespan and low resistance to fouling [3, 4]. In this context,

ceramic membranes are increasingly gaining popularity due to several advantages such as controlled distribution of pore size, high porosity and separation capability, hydrophilicity, and superior thermal, mechanical, and chemical stability [5, 6].

Ceramic membranes are commonly made from metal oxides such as ZrO_2, TiO_2, and SiO_2. Their advantages include a longer service life and reduced fouling compared to polymeric membranes [7-9]. However, metal oxide ceramic membranes have drawbacks, including high cost and brittleness. Recently, researchers have been working on reducing the cost of ceramic membranes by incorporating low-cost natural clay minerals into the initial mix. The use of these additives can significantly lower the production costs of ceramic membranes without compromising their quality [10, 11].

In [12], tubular ceramic membranes based on kaolinite with the addition of calcium carbonate were investigated. The authors established that the compressive strength of the samples gradually increased with the sintering temperature up to 1200 °C, after which it remained constant (around 40 MPa). Another study [13] demonstrated the possibility of creating composite membranes based on aluminium oxide and kaolin. It was found that increasing the kaolin content positively influenced the flexural strength limit. Samples fired at 1450 °C had strengths ranging from 2.7 to 14 MPa, depending on the increase in kaolin content from 10% to 50%. Therefore, further strength enhancement can be achieved by adding various materials, such as calcium-containing materials, silicon carbide, or other substances [14, 15].

The study [16] also presented the positive effect of kaolin on the mechanical properties of composite membranes. The kaolin content in the aluminium oxide/kaolin system ranged from 75% to 87.5%, with compressive strength ranging from 13 MPa to 38 MPa. The results show that increasing the kaolin content reduces the firing temperature of the samples while maintaining their mechanical strength. Additionally, high values of flexural strength for kaolin-based ceramic membrane samples were demonstrated in [17].

The effect of sintering temperature on the mechanical properties of kaolin-based membranes was examined in [18]. There was a tendency for increasing mechanical strength from 5 MPa to 127 MPa with rising the firing temperature from 1200 °C to 1500 °C. In addition, the formation of a greater number of new bonds between ceramic particles leads to an overall increase in the mechanical strength of the membrane.

The study [19] presented the studies of the mechanical properties of membranes based on a complex mixture containing kaolin, quartz, calcium carbonate, sodium carbonate, boric acid, and sodium metasilicate. It was established that increasing the firing temperature from 850 °C to 1000 °C leads to an increase in flexural strength from 3 MPa to 8 MPa. Thus, a significant effect of the sintering temperature on the strength of ceramic membranes was observed.

Taking these data into account, the study of the influence of the sintering temperature regime on the ceramic matrix, as well as the determination of the influence of the components of the initial mixture on the physicochemical and mechanical properties is extremely relevant. This will allow optimizing rational parameters for creating inexpensive ceramic membranes based on clay minerals, in particular kaolin and saponite. It should be added that there are virtually no studies in the literature on the production of ceramic membranes using saponite clay, which further emphasizes the relevance of this study.

The study aimed to investigate the influence of sintering temperature and phase composition of the initial mixture on the physicochemical, mechanical and transport properties of ceramic membranes based on kaolin and saponite.

2. Experimental

Materials

For the synthesis of ceramic membranes, the following materials were used: kaolin ($Al_2O_3 \cdot 2SiO_2 \cdot 2H_2O$, Glukhovetske field, Vinnytsia region, Ukraine), saponite ($NaMg_3[AlSi_3O_{10}](OH)_2 \cdot 4H_2O$, Tashkivske field, Khmelnytskyi region, Ukraine), silicon carbide (SiC), calcium carbonate ($CaCO_3$), and sodium silicate (Na_2SiO_3).

Synthesis procedures

To obtain ceramic matrices, a fraction ≤ 40 μm of the main components (kaolin, saponite and silicon carbide) was used. The choice of this particular fraction was based on literature sources [20]. A series of matrices with varying contents of kaolin (from 30 wt% to 60 wt%) and silicon carbide (from 0 wt% to 30 wt%) were prepared using the dry pressing method fol-

Table 1. Percentage compositions of ceramic membrane matrix samples and sintering temperature

№	Sample	Sintering temperature, °C	Kaolin	Saponite	Na_2SiO_3	$CaCO_3$	SiC
1	CM1/800	800	60	10	10	20	0
2	CM2/800		50				10
3	CM3/800		40				20
4	CM4/800		30				30
5	CM1/950	950	60	10	10	20	0
6	CM2/950		50				10
7	CM3/950		40				20
8	CM4/950		30				30
9	CM1/1100	1100	60	10	10	20	0
10	CM2/1100		50				10
11	CM3/1100		40				20
12	CM4/1100		30				30

lowed by sintering at temperatures of 800 °C, 950 °C, and 1100 °C. For this, the respective materials were ground, weighed, and mixed in specific proportions. The resulting powder was then pressed into a mold using a manual hydraulic press under a pressure of 10 tons.

The compositions of the initial mixtures for obtaining ceramic membrane matrices are presented in Table 1.

After the pressing stage, the formed matrices were sintered at temperatures of 800 °C, 950 °C, and 1100 °C to enhance their strength. The thermal treatment was conducted in an air atmosphere in a high-temperature muffle furnace. The heating rate was set to 1°/min up to 95 °C with an isothermal hold for 30 minutes, then at a heating rate of 3°/min up to 350 °C, and finally at a heating rate of 2°/min up to 800 °C/950 °C/1100 °C, with a subsequent hold at this temperature for 60 minutes. The samples were then cooled to room temperature and tested.

Material Characterization

The content of chemical elements in clays was determined by measuring the mass fraction of chemical elements in the samples using the non-destructive energy dispersive X-ray fluorescence analysis with a precision analyser EXPERT 3L, INAM (Ukraine). The range of detectable chemical elements (control range) spanned from magnesium (12Mg) to uranium (92U). The measurement range of mass fractions (concentrations) of elements varied from 0.005% to 100%. The samples of ceramic membrane matrices were studied using X-ray phase analysis on a Rigaku Ultima IV diffractometer (Japan) with copper radiation (CuKα = 0.15418 nm, 40 kV, 30 mA). The phase composition and average crystallite size were automatically calculated using the PDXL software application based on standard cards (ICDD and PDF-2/Release 2011 RDB databases). Infrared transmission spectra were recorded using a Fourier-transform infrared spectrometer IRAffinity–1S (Shimadzu, Japan) in the range of 4000–400 cm^{-1} (number of scans – 32, resolution – 4 cm^{-1}). Thermal analysis of the studied samples was carried out in an air environment using a Derivatigraf Q–1500 thermoanalyzer (MOM, Hungary). Samples were placed in a platinum crucible, with calcined Al_2O_3 as a reference.

Porosity characteristics

Nitrogen adsorption isotherm data were collected at 77 K on a NOVAtouch 4200e (Quantachrome Instruments) surface area and pore-size analyser. The specific surface areas were determined using the Brunauer-Emmett-Teller (BET) method and the BET equation was used to fit data from the linear region of the adsorption branch according to [21]. The pore sizes were determined using the Barrett-Joyner-Halenda (BJH) method.

Mechanical properties

To determine the flexural strength, the standardized method DSTU ISO 14704:2006 "High-quality ceramic products (ceramics and technical ceramics of improved type)" was used. According to the method, the flexural strength

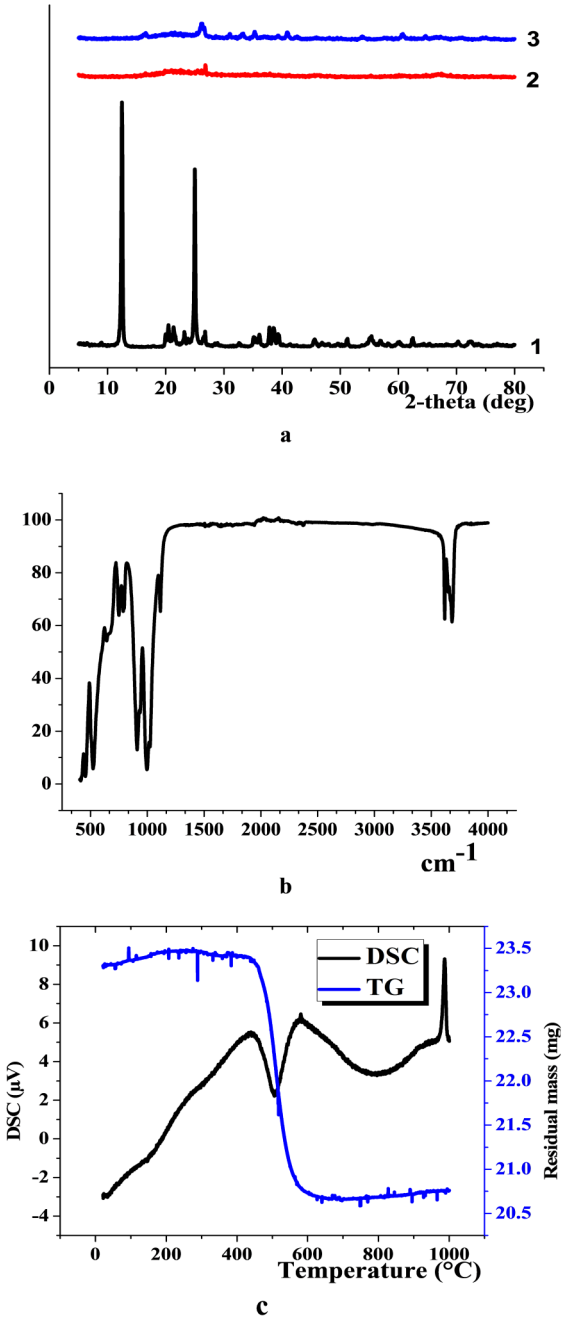

Fig. 1. X-ray diffraction patterns (a) of raw (1) and heat-treated kaolin samples (2 – 950 °C, 3 – 1100 °C), FTIR spectrum (b) and thermogram (c) of raw kaolin.

of the samples was measured using a three-point scheme (Bending strength tester, BTS 401/3, Netzsch, Germany) with a sample length of 50 mm, width of 10 mm, and height of 2 mm at a load of 1 N.

Electrical properties

Streaming potential was determined using the laboratory setup. The experimental setup included two 200 ml containers separated by a ceramic membrane, hermetically sealed with rubber gaskets. Silver chloride reference electrodes were placed on each membrane side, connected to a high-resistance voltmeter. Both containers contained a 0.02 mol/L KCl solution. The upper container was sealed airtight, with a rubber bulb for pressure generation and a mercury manometer for pressure measurement. After filling both containers with the solution, the initial voltage across the electrodes at atmospheric pressure was recorded. An overpressure of 200 mm·Hg was then created in the upper container using the bulb. The voltage was noted every 20 mm·Hg as the pressure decreased. This process was repeated three times for each membrane. Data demonstrating potential differences depending on the applied pressure were presented graphically. The uniqueness of this method lies in the fact that measurements are carried out during filtration, which increases simplicity and realism.

Transport properties

The transport properties of the ceramic membrane matrix were investigated by measuring the permeability to pure water using an original laboratory setup. For this purpose, these membranes were cleaned with water, then with ethanol in an ultrasonic bath. After cleaning, they were dried in an oven at 60 °C. The cleaned and dried membranes were positioned in a special cell. Water was pumped through this cell, and the pressure at which water permeated the membrane was monitored using a pressure gauge. Additionally, the volume of water filtered through the membrane per minute was measured.

3. Results and discussion

Physicochemical properties of raw materials

Initially, the clay components (kaolin and saponite) of the ceramic membrane matrix were identified. The raw and thermally treated kaolin and saponite, subjected to various temperatures, were analysed using X-ray fluorescence analysis, diffraction methods, infrared spectroscopy, and thermal analysis.

Native kaolin contains the following chemical elements: Si (58.4%), Al (33.9%), Ti (3.3%), and Fe (2.4%) as the main elements, along with Mg, Ca, S, V, Cr, Ga, Zr, and Pb as elements present at 1% and below.

Fig. 1a shows X-ray diffraction patterns of the raw kaolin and kaolin thermally treated

Table 2. Structural-adsorption characteristics of raw and heat-treated kaolin samples

Parameters	Raw kaolin	Kaolin-950	Kaolin–1100
$S_{specific}$, $m^2 \cdot g^{-1}$ (BET)	8	13	6
$V_{mesopor}$, $sm^{3} \cdot g^{-1}$	0.052	0.036	0.025
D, nm	3.9	3.9	3.1

at 950 °C and 1100 °C. Using the software, the raw kaolin was identified as a mixture of kaolinite $Al_4(OH)_8(Si_4O_{10})$ and quartz; the sample thermally treated at 950 °C contained an amorphous phase (metakaolinite) and quartz; and the sample treated at 1100 °C was a mixture of an amorphous phase, quartz SiO_2 and mullite $Al(Al_{.83}Si_{1.08}O_{4.85})$.

In the FTIR spectrum of raw kaolin (Fig. 1b), bands are clearly visible at 3684 cm^{-1}, 3671 cm^{-1}, 3651 cm^{-1}, and 3618 cm^{-1}, indicating an ordered structure of kaolinite in the range of 3684-3618 cm^{-1}. The bands at 3684 cm^{-1}, 3671 cm^{-1}, and 3651 cm^{-1} are due to surface hydroxyl groups creating valence vibrations of O-H, and the band at 3618 cm^{-1} is related to valence vibrations of OH in the internal hydroxyl group [22].

The thermogram of native kaolin (Fig. 1c) shows a sharp mass loss at 450 °C, due to the process of dehydroxylation (loss of structural water) [23]:

$$Al_2O_3 \cdot 2SiO_2 \cdot 2H_2O \rightarrow Al_2O_3 \cdot 2SiO_2 + 2H_2O.$$

Further heating to 600 °C leads to the appearance of an exothermic peak, signifying the formation of metakaolin. Additionally, an exothermic peak observed at 930-950 °C on the DSC curve corresponds to the formation of mullite [23]:

$$3(Si_3Al_4O_{12}) \rightarrow 2(Si_2Al_6O_{13}) + 5SiO_2.$$

These findings confirm the obtained phase composition for kaolin samples thermally treated at 950 °C and 1100 °C.

The obtained structural and adsorption characteristics of samples of raw and heat-treated kaolin are given in Table 2. The nitrogen adsorption-desorption isotherms are shown in Fig. 2. The isotherms of all kaolin samples are concave to the p/p_0 axis over the entire range and belong to type III, indicating that the samples are either macroporous or non-porous with minor mesoporosity [24], as confirmed by the pore diameter values (Table 2).

The data presented in Table 2 shows that the specific surface area of the untreated kaolin samples is 8 $m^2 \cdot g^{-1}$, while for those heat-treat-

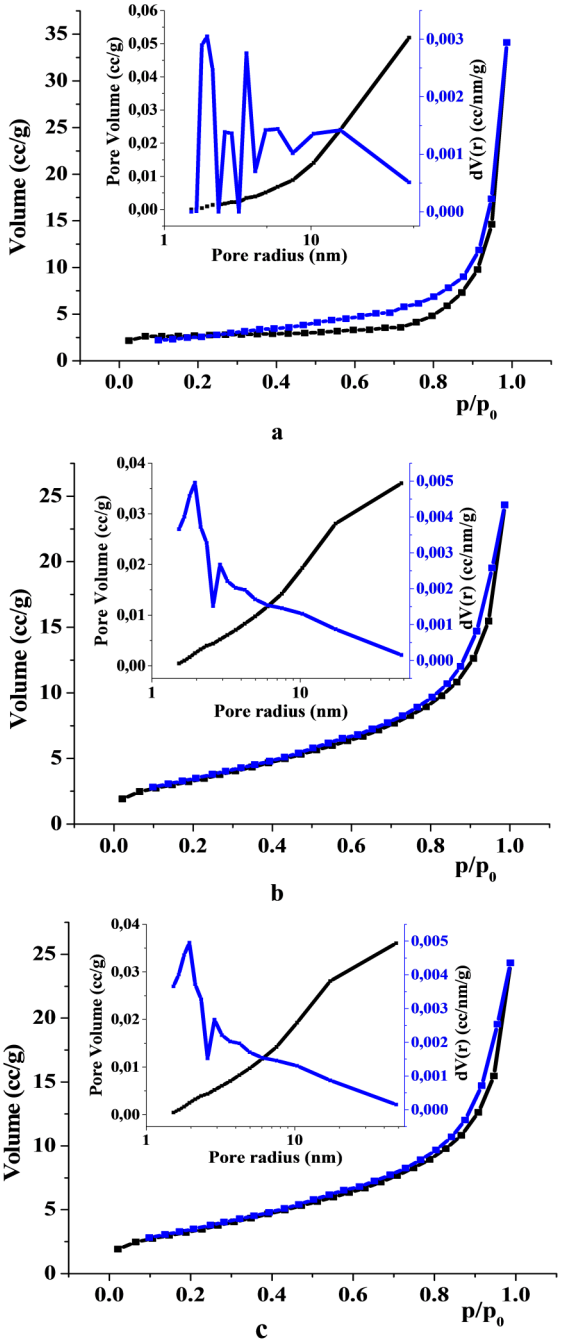

Fig.2. Nitrogen adsorption-desorption isotherms and pore size distribution for kaolin samples: a – raw kaolin, b – kaolin treated at 950 °C, c – kaolin treated at 1100 °C.

Table 3. Structural-adsorption characteristics of saponite samples.

Parameters	Raw saponite	Saponite–1100
$S_{specific}$, $m^2 \cdot g^{-1}$ (BET)	12	0.3
$V_{mesopor}$, $sm^3 \cdot g^{-1}$	0.029	0.001
D, nm	3.96	3.62

ed at 950 °C and 1100 °C, it is 13 $m^2 \cdot g^{-1}$, and 6 $m^2\ g^{-1}$, respectively. Small changes in the structural and adsorption characteristics of kaolin samples can be explained by phase transformations of kaolin during heat treatment.

Chemical elements included in saponite clay: Si (61.32%), Ca (12.07%), K (10.3%), Fe (7.37%), and Al (6.09%) as the main elements, and Mg, Ti, S, Mn, Sr, Rb, Zr, Zn, and Pb as elements present at levels of 4% and below.

Saponite samples were analysed using the XRD method before and after sintering at a temperature of 1100 °C. The raw saponite sample was identified as a mixture of saponite $NaMg_3[AlSi_3O_{10}](OH)_2 \cdot 4H_2O$ and quartz SiO_2 (ICDD standard cards 00-030-0789 (PDF) and 01-087-2096 (PDF-2), respectively). The saponite sample heat-treated at 1100 °C was identified as a mixture of phases with the structure of enstatite $Mg_2(Si_2O_6)$ and cristobalite SiO_2 (high-temperature modification of quartz), which was determined from standard cards 9001641 and 1010954 of COD database for enstatite and cristobalite, respectively (Fig. 3a).

The FTIR spectrum of saponite (Fig. 3b) indicates the presence of various types of structural bonds and functional groups. The high-frequency region of the spectrum contains an overlapping broad absorption band in the range of 3700-3000 cm^{-1}, corresponding to the valence vibration of hydroxyl groups. An intense band at about 3588 cm^{-1} corresponds to the valence vibration of OH groups in the Mg–OH–Fe bonds of the trioctahedral layers. The absorption band around 3386 cm^{-1} may be associated with valence vibrations of OH bonds in Fe–OH–Fe and indicates isomorphic substitution of Fe for Mg in the trioctahedral layers of Fe saponite. The absorption band at 1638 cm^{-1} is related to the deformation of molecular water H–O–H. An intense absorption band with a peak at about 982 cm^{-1} corresponds to the vibration of O–Si–O, which is part of the tetrahedral layer. Absorption bands at 797 cm^{-1} and 727 cm^{-1} were caused by out-of-plane vibrations of Fe–OH–Fe and Fe–O, respectively. A small peak at 511 cm^{-1} is associated with the defor-

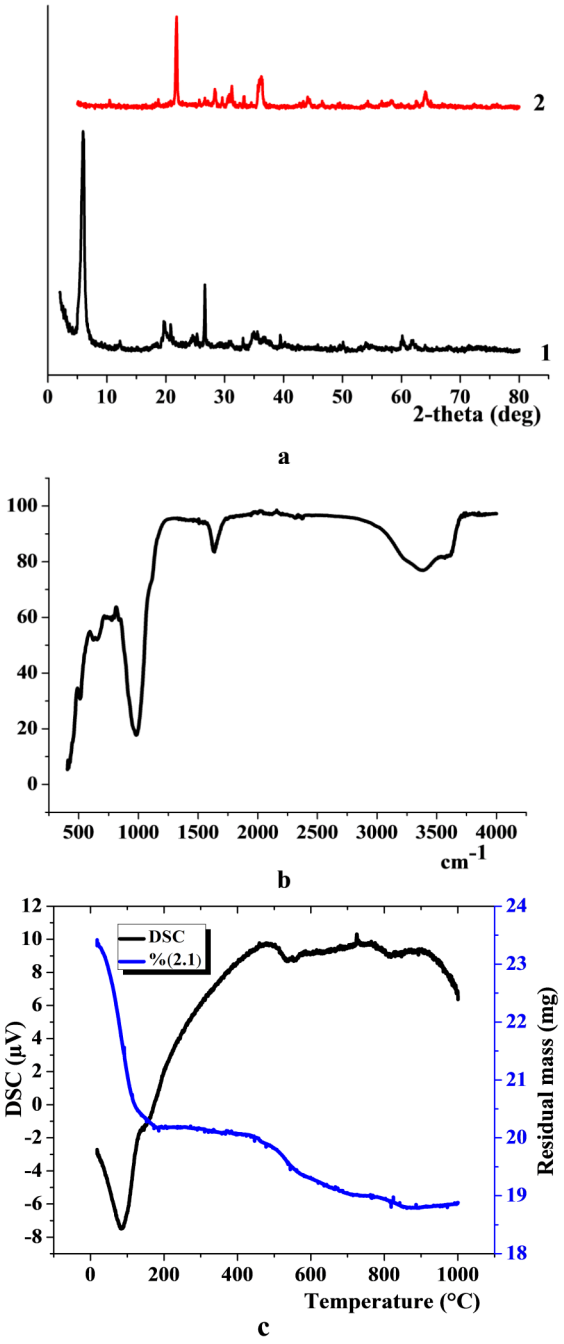

Fig. 3. X-ray diffraction patterns (a) of native (1) and heat-treated saponite samples (2 – 1100 °C), FTIR spectrum (b) and thermogram (c) of native saponite.

mation of Si–O–Al and indicates the presence of some aluminium in the tetrahedral layer [25],[26].

The analysis of the saponite (heating up to 1000 °C) thermogram (Fig. 3c) indicates the removal of weakly bound water, starting at room temperature and ending at 200 °C, which is confirmed by the corresponding endothermic peak with a maximum at 95 °C. The removal of strongly bound interlayer water occurs between 200 °C and 400 °C, after which the process of dehydroxylation of the saponite structure begins at 400-700 °C; this probably leads to the formation of the enstatite phase [27]. Subsequently, no mass loss of the saponite sample was observed with increasing temperature.

The investigated structural-adsorption characteristics of saponite before and after sintering are presented in Table 3, and the nitrogen adsorption-desorption isotherms as well as the distribution of the specific surface area of mesopores are shown in Figure 4. Table 6 shows that the specific surface area of untreated saponite samples is 12 $m^2 \cdot g^{-1}$; while for heat-treated samples, it is 0.3 $m^2 \cdot g^{-1}$. This indicates the process of pore coalescence, which occurs at a temperature of 1100 °C.

The isotherms of raw saponite and samples heat-treated at 1100 °C have a similar shape and belong to type IV, i.e., they are mesoporous. However, the appearance of the hysteresis loop on the corresponding isotherms confirms the coalescence of mesopores.

Physicochemical properties of ceramic matrices

The obtained X-ray diffraction patterns for all ceramic membrane matrices SM–1, SM-2, SM-3, and SM-4 show that all samples except SM1 sintered at 800 °C, have the same phase composition: silicon carbide, calcium oxide, calcite, and quartz. The matrices heat-treated at 950 °C have a slightly different composition: silicon carbide, calcium oxide, quartz, mullite. All samples sintered at the temperature of 1100 °C have the following phase composition: silicon carbide, mullite, calcium oxide, and albite. Additionally, it can be noted that the samples heat-treated at 800 °C and 950 °C contain an amorphous phase, which is a result of the transformation of kaolinite into amorphous metakaolinite at these sintering temperatures.

Mechanical properties

The use of kaolin as the primary raw material requires extremely high sintering temperatures to ensure complete phase transformations and sintering reactions. The introduction of additional components into the press-powder, such as saponite, sodium silicate, calcium carbonate, and silicon carbide, reduce the sintering temperature due to the formation of low-melting eutectics and improve their mechanical characteristics.

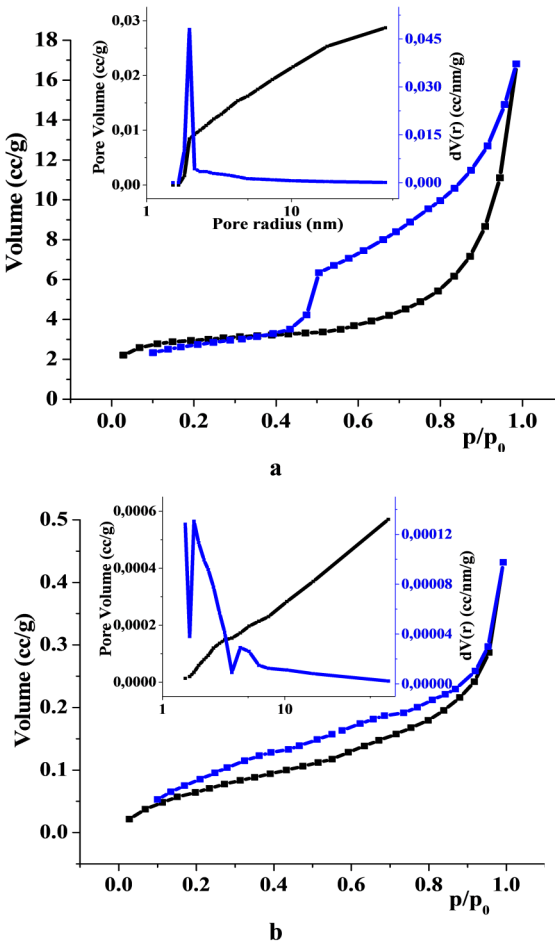

Fig. 4. Nitrogen adsorption-desorption isotherms and pore size distribution for saponite samples: a – raw saponite, b – saponite sintered at 1100 °C.

The results of determining the flexural strength for all synthesised samples of ceramic membrane matrices are presented in Fig. 5. A pressure of 20 MPa was used to press the ceramic matrices.

As can be seen, an increase in sintering temperature from 800 °C to 1100 °C leads to a consistent increase in the flexural strength. The curves at 800 °C and 950 °C are extreme and, to some extent, indicate that the optimal kaolin content is 40%. An increase in the SiC content leads to an increase in the strength of ceramic membranes [28]. The dependence of strength

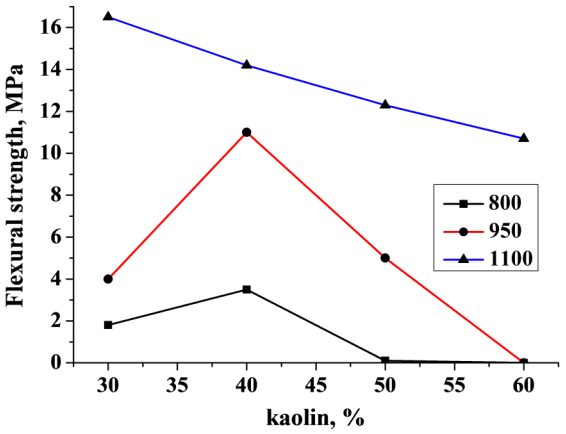

Fig. 5. Flexural strength depending on kaolin content for different sintering temperatures

on kaolin content for samples heat-treated at 1100 °C shows an almost proportional relationship between strength and kaolin and SiC content, which is probably due to phase transformations of kaolinite and saponite and the formation of a greater number of chemical bonds in the system.

Considering the measurement results, the optimal sintering temperature should be 950–1100 °C, which should ensure higher sample strength. Accordingly, based on the obtained data, only samples produced at 950 °C and 1100 °C were further studied.

Electrical properties

The surface charge of membranes is an essential factor for interpreting and predicting their properties in the filtration process, such as resistance to biofouling, etc. The electrokinetic properties were studied by the streaming potential method using silver chloride electrodes. The magnitude of the tangent of the slope angle $\Delta E/\Delta P$ (streaming potential) was used to determine the sign of the surface charge and to calculate the ζ-potential using the Smoluchowski equation [23].

The obtained relationships for all studied ceramic membrane matrices showed a linear increase in the streaming potential with increasing applied pressure. This indicates that concentration polarisation within this range of pressures does not affect the performance of these membranes. However, the value of the potential E (mV) significantly depended on the composition of the membrane. Based on the determined streaming potential and an additional experimental study of the electrical conductivity of the membranes, the ζ-potential was calculated (Table 4).

Table 4. Streaming potential ($\Delta E/\Delta P$) and ζ-potential of the membranes

Sample	ΔE/ΔP	ζ, mV
CM1/950	-0.00015	–15.2
CM2/950	-0.00025	-24.3
CM3/950	-0.00024	-22.7
CM4/950	-0.00028	-27.1
CM1/1100	-0.00017	–16.3
CM2/1100	0.00011	10.3
CM3/1100	0.00010	9.7
CM4/1100	0.00011	10.9

Table 5. Permeability of ceramic membrane matrices

Sample	Pure water permeability, $cm^3/(min \cdot cm^2)$
CM1/950	9.5
CM2/950	11.1
CM3/950	12.5
CM4/950	14.0
CM1/1100	8.4
CM2/1100	9.3
CM3/1100	9.9
CM4/1100	11.2

The results show a negative value of the ζ-potential obtained for all ceramic membrane matrices heat-treated at 950 °C and CM1/1100. This indicates that these matrices will be more resistant to fouling during operation.

Transport properties

The permeability values to pure water of ceramic matrices are shown in Table 5. As can be seen, the synthesised ceramic membranes filter pure water at zero pressure, indicating their macroporosity [29].

To confirm the macroporous structure of the obtained ceramic matrices, their surface was additionally examined by scanning electron microscopy. SEM images of the ceramic matrices are shown in Figure 6.

As can be seen from Figure 6, all ceramic matrices have pores ranging in size from approximately 10 μm to 200 μm, which confirms the macroporosity of the ceramic matrices.

The data in Table 5 indicate that the permeability depends on the sintering temperature and composition of the ceramic membranes: with an increase in the sintering temperature, the permeability decreases, while a decrease in the kaolin content (increase in the silicon carbide content) leads to an increase in permeability. In pure water, the permeability varies from

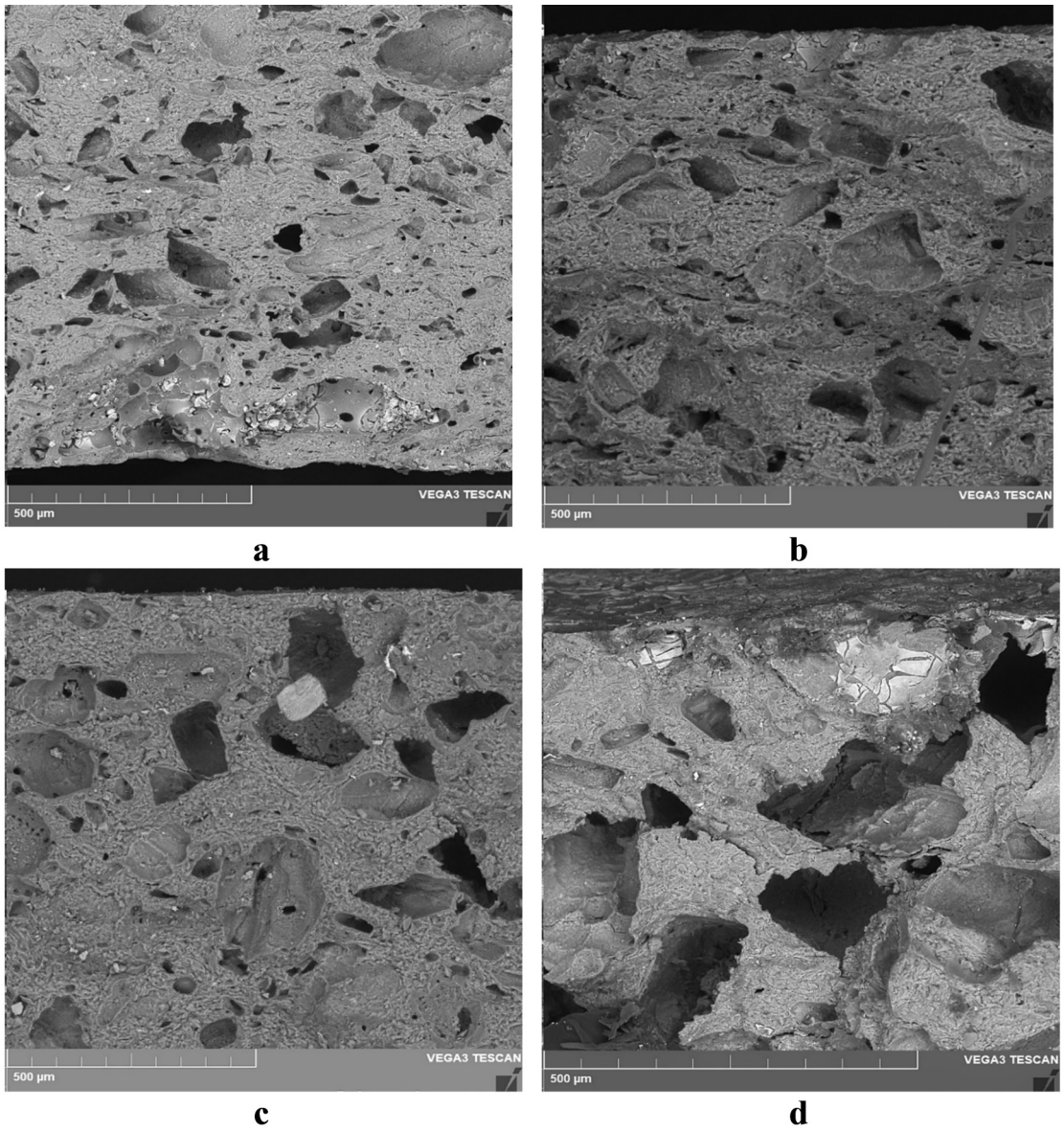

Fig. 6. SEM images of ceramic matrix samples: a – CM–1, b – CM-2, c – CM-3, d – CM-4.

8.4 $cm^3/(min \cdot cm^2)$ to 14 $cm^3/(min \cdot cm^2)$, which are fairly high values for the obtained ceramic membranes. The porosity determined for all the ceramic membranes studied ranges from 44% to 65% according to ISO 14704:2000, indicating the high permeability of these membranes.

4. Conclusions

The study demonstrates the high potential of creating ceramic membranes using natural raw materials, particularly kaolin and saponite clays, as a cost-effective approach for their use in water purification. It has been established that the sintering temperature and phase composition significantly affect the mechanical and transport properties of ceramic membranes. Some processes have been identified that also occur during the synthesis of ceramic membrane matrices. A significant influence of temperature and composition of the initial mixture on the flexural strength was established; for the selected ceramic matrices the flexural strength is in the range of 10–16 MPa. The electrical properties suggest potential resistance to fouling during operation. The obtained ceramic membrane matrices were found to have a macroporous structure, high porosity (44-65%) and fairly high permeability for pure water.

Acknowledgments

We are grateful to the National Research Foundation of Ukraine for funding the project (project registration number 2020.02/0024).

References

1. M. Sheikh, M. Pazirofteh, M. Dehghani, M. Asghari, M. Rezakazemi, C. Valderrama, J.L. Cortina, *Chem. Eng. J.,* **391**, 123475 (2020)
2. X. Xu, Y. Yang, T. Liu, B. *Chu. Giant.* **10**, 100099 (2022)
3. J. Schnittger, J. McCutcheon, T. Hoyer, M. Weyd, G. Fischer, P. Puhlfürß, M. Halisch, I. Voigt, A. Lerch, *J. Memb. Sci.* **618**, 118678 (2021)
4. C.S. Raota, S. Lotfi, R. Lyubimenko, B.S. Richards, A.I. Schäfer, *J. Memb. Sci.* **686**, 121944 (2023)
5. Z. He, Z. Lyu, Q. Gu, L. Zhang, J. Wang, Colloids Surfaces A Physicochem. *Eng. Asp.*, **578**, 123513 (2019)
6. M.B. Asif, , Z. Zhang, *Chem. Eng. J.*, **418**, 129481 (2021)
7. C. Li, W. Sun, Z. Lu, X. Ao, S. Li, *Water Res.*, **175**, 115674 (2020)
8. B. Jafari, E. Rezaei, M.J. Dianat, M. Abbasi, S.A. Hashemifard, A. Khosravi, M. Sillanpää, *Ceram. Int.,* **47**, 24 (2021)
9. N.M.A. Omar, M.H.D. Othman, Z.S. Tai, T.A. Kurniawan, T. El-badawy, P.S. Goh, N.H. Othman, M.A. Rahman, J. Jaafar, A.F. Ismail, *J. Eur. Ceram. Soc.,* **42**, 13 (2022)
10. A. Elgamouz, N. Tijani, *Microporous Mesoporous Mater.*, 271 (2018)
11. Samadi, A., Gao, L., Kong, L., Orooji, Y., Zhao, S., *Resour. Conserv. Recycl.*, **185,** 106497 (2022)
12. B. Ghouil, A. Harabi, F. Bouzerara, B. Boudaira, A. Guechi, M.M. Demir, A. Figoli, *Mater. Charact.*, **103** (2015)
13. L.F. Han, Z.L. Xu, Y. Cao, Y.M. Wei, H.T. Xu, *J. Memb. Sci.*, **372** (2011)
14. J.B. Kowalska, T. Zaleski, A. Józefowska, R. Mazurek, *Catena*, **174** (2019)
15. E. Eray, V.M. Candelario, V. Boffa, H. Safafar, D.N. Østedgaard-Munck, N. Zahrtmann, H. Kadrispahic, M.K. Jørgensen, *Chem. Eng. J.,* **414**, 128826 (2021)
16. I. Hedfi, N. Hamdi, M.A. Rodriguez, E. Srasra, *Ceram. Int.*, **42,** 4 (2016)
17. S.K. Hubadillah, M.H.D. Othman, A.F. Ismail, M.A. Rahman, J. Jaafar, *J. Teknol.,* **79** (2017)
18. N.H. Mohtor, M.H.D. Othman, A.F. Ismail, M.A. Rahman, J. Jaafar, N.A. Hashim, *Environ. Sci. Pollut. Res.*, **24** (2017)
19. B.K. Nandi, R. Uppaluri, M.K. Purkait, *Appl. Clay Sci.*, **42** (2008)
20. S. Rajpoot, J.-H. Ha, , Y.-W. Kim, *Ceram. Int.,* **47**, 6, (2021)
21. O.I. Yanushevska, T.A. Dontsova, A.I. Aleksyk, N.V. Vlasenko, O.Z. Didenko, A.S. Nypadymka, *Clays Clay Miner.*, **68**, 5 (2020)
22. B.J. Saikia, G. Parthasarathy, *J. Mod. Phys.*, **01** (2010)
23. A.O. Serhiienko, T.A. Dontsova, O.I. Yanushevska, V.I. Vorobyova, G.S. Vasyliev, *Mol. Cryst. Liq. Cryst.*, **752** (2023)
24. M. Thommes, K. Kaneko, A.V. Neimark, J.P. Olivier, F. Rodriguez-Reinoso, J. Rouquerol, K.S.W. Sing, *IUPAC Technical Report, Pure Appl. Chem.*, **87** (2015)
25. N. Mykhailenko, O. Makarchuk, T. Dontsova, S. Gorobets, I. Astrelin, Eastern-European *J. Enterp. Technol.*, **4**, 76 (2015)
26. H. Sokol, M. Sprynskyy, A. Ganzyuk, V. Raks, B. Buszewski, *Colloids and Interfaces*, 3 (2019)
27. I. Ohnishi1, K. Tomeoka, *Meteorit. Planet. Sci.,* **42**, 1, (2007)
28. J. Wang, X. Wang, Q. Fu, J. Fu, F. Zhai, Shuang Li, *Ceram. Int.*, **49**, 15 (2023)
29. Zhou Zhentao, A. Sukhoivanenko, T. Dontsova, *Funct. Mater.* **31** (4): 630, 2024.